

Preparation, Structural Characterization, and Antifungal Activities of Complexes of Group 12 Metals with 2-Acetylpyridine- and 2-Acetylpyridine-N-oxide-⁴N-phenylthiosemicarbazones

Elena Bermejo, Alfonso Castiñeiras*, Ricardo Domínguez

Santiago de Compostela/Spain, Universidad de Santiago de Compostela. Departamento de Química Inorgánica

Rosa Carballo

Vigo/Spain, Universidad de Vigo, Departamento de Química Inorgánica

Cäcilia Maichle-Mössmer, Joachim Strähle

Tübingen/Germany, Institut für Anorganische Chemie der Universität

Douglas X. West

Normal/USA, Illinois State University, Department of Chemistry

Received January 14th, 1999.

Abstract. Reaction of group 12 metal dihalides in ethanolic media with 2-acetylpyridine-⁴N-phenylthiosemicarbazone (**H4PL**) and 2-acetylpyridine-N-oxide-⁴N-phenylthiosemicarbazone (**H4PLO**) afforded the compounds [M(H4PL)X₂] (X = Cl, Br, M = Zn, Cd, Hg; X = I, M = Zn, Cd) (**1–8**), [Hg(4PL)I]₂ (**9**) and [M(H4PLO)X₂] (X = Cl, Br, I, M = Zn, Cd, Hg) (**10–18**). **H4PL**, **H4PLO** and their complexes were characterized by elemental analysis and by IR and ¹H and ¹³C NMR spectroscopy (and the cadmium complexes by ¹¹³Cd NMR spectroscopy), and **H4PL**, **H4PLO**, (**5 · DMSO**) and (**9**) were additionally studied by X-ray diffraction.

H4PL is N,N,S-tridentate in all its complexes, including **9**, in which it is deprotonated, and **H4PLO** is in all cases O,N,S-tridentate. In all the complexes, the metal atoms are pentacoordinate and the coordination polyhedra are redistorted tetragonal pyramids. In assays of antifungal activity against *Aspergillus niger* and *Paecilomyces variotii*, the only compound to show any activity was [Hg(H4PLO)I₂] (**18**).

Keywords: Cadmium; Mercury; Zinc; 2-Acetylpyridine-⁴N-phenylthiosemicarbazone; 2-acetylpyridine-N-oxide-⁴N-phenylthiosemicarbazone; ¹¹³Cd NMR

Synthese, strukturelle Charakterisierung und fungizide Eigenschaften von Komplexen mit 2-Acetylpyridin- und 2-Acetylpyridin-N-oxid-⁴N-phenylthiosemicarbazon der Metalle der 12. Gruppe

Inhaltsübersicht. Bei der Umsetzung von Zn-, Cd- und Hg-Halogeniden in Ethanol mit den Thiosemicarbazonen: 2-Acetylpyridine-⁴N-phenylthiosemicarbazon (**H4PL**) und 2-Acetylpyridine-N-oxide-⁴N-phenylthiosemicarbazon (**H4PLO**) erhält man die Verbindungen [M(H4PL)X₂] (X = Cl, Br, M = Zn, Cd, Hg; X = I, M = Zn, Cd) (**1–8**), [Hg(4PL)I]₂ (**9**) und [M(H4PLO)X₂] (X = Cl, Br, I, M = Zn, Cd, Hg) (**10–18**). Die Charakterisierung und Strukturen der Liganden und der Komplexe wurde mit Hilfe von Elementaranalysen, ¹H, ¹³C, ¹¹³Cd NMR- und von IR-Spektren durchgeführt. Die Strukturen von **H4PL**, **H4PLO**, **5 · DMSO** und **9** wurden durch Einkristallröntgenstrukturanalyse be-

stimmt. In **9** liegt **H4PL**, in deprotonierter Form, als NNS-dreizähniger Ligand vor, während er in den anderen Komplexen als neutraler Ligand koordiniert. Die Metallkomplexe mit **H4PLO** als Ligand zeigen eine ONS-dreizähnige Koordination ohne Deprotonierung. Das Zentralatom hat in allen hier vorgestellten Komplexen die Koordinationszahl fünf mit verzerrt tetragonal-pyramidalen Koordinationspolyedern. Für die Thiosemicarbazone und deren Komplexe wurde die fungizide Aktivität gegen *Aspergillus niger* und *Paecilomyces variotii* getestet, jedoch zeigte nur [Hg(H4PLO)I₂] (**18**) Aktivität.

* Prof. Dr. A. Castiñeiras
Departamento de Química Inorgánica
Facultad de Farmacia
Universidad de Santiago de Compostela
E-15706 Santiago de Compostela/Spain
Fax: +34 981 54 71 63
E-mail: qiac01@usc.es

Introduction

The thiosemicarbazones 2-acetylpyridine- and 2-acetylpyridine-N-oxide-⁴N-phenylthiosemicarbazones as well as their complexes with metals are biologically

Table 1 Analytical data, colours, melting points and yields of complexes of Zn, Cd, and Hg with **H4PL** and **H4PLO**^{a)}

No.	Compound	Colour	Mp. (°C)	%C	%H	%N	Yield (%)
1	[Zn(H4PL)Cl ₂]	yellow	300*	41.4(41.4)	3.4(3.5)	13.6(13.8)	69
2	[Zn(H4PL)Br ₂]	yellow	302	34.1(33.9)	2.7(2.8)	11.3(11.1)	73
3	[Zn(H4PL)I ₂]	yellow	281*	29.5(28.5)	2.3(2.4)	9.5(9.5)	73
4	[Cd(H4PL)Cl ₂]	yellow	295	37.3(37.1)	3.0(3.1)	12.1(12.4)	76
5	[Cd(H4PL)Br ₂]	yellow	296	30.9(30.5)	2.5(2.5)	10.0(10.2)	76
6	[Cd(H4PL)I ₂]	yellow	283	26.8(26.4)	2.2(2.2)	8.7(8.8)	78
7	[Hg(H4PL)Cl ₂]	yellow	234	31.1(31.0)	2.5(2.6)	10.1(10.3)	76
8	[Hg(H4PL)Br ₂]	yellow	241	26.7(26.7)	2.1(2.2)	8.6(8.9)	71
9	[Hg(4PL)I ₂]	yellow	133	24.0(23.2)	2.1(1.9)	7.3(7.7)	68
10	[Zn(H4PLO)Cl ₂]	yellow	257	39.4(39.8)	3.4(3.3)	13.2(13.3)	63
11	[Zn(H4PLO)Br ₂]	yellow	273	33.9(32.9)	2.7(2.7)	11.0(11.0)	69
12	[Zn(H4PLO)I ₂]	yellow	195	27.6(27.8)	2.1(2.3)	8.9(9.3)	69
13	[Cd(H4PLO)Cl ₂]	yellow	228	34.7(35.8)	3.1(3.0)	11.1(11.9)	77
14	[Cd(H4PLO)Br ₂]	yellow	224	30.2(30.1)	2.6(2.5)	9.9(10.0)	73
15	[Cd(H4PLO)I ₂]	yellow	206	26.0(25.8)	2.2(2.2)	8.7(8.6)	75
16	[Hg(H4PLO)Cl ₂]	orange	213	29.4(30.1)	2.2(2.5)	9.9(10.0)	76
17	[Hg(H4PLO)Br ₂]	brown	260*	25.7(26.0)	2.0(2.2)	8.6(8.7)	67
18	[Hg(H4PLO)I ₂]	yellow	189	22.3(22.7)	1.5(1.9)	7.2(7.6)	82

^{a)} In parentheses, calculated values; *Decomposition

and pharmacologically active [1], and have been the object of a considerable amount of research. There have nevertheless been relatively few studies of the coordination of thiosemicarbazones to non-transition metals, and of the biological activity of the resulting coordination compounds [2–4]. The complexes of thiosemicarbazones with group 12 metals constitute an especially attractive topic in view of the marked differences among group 12 metals as regards both chemical behaviour and biological activity (Zn^{II} is an essential element because of its presence in certain metalloenzymes, while the capacity of Cd^{II} and Hg^{II} for coordination to biomolecules makes them rank among the most toxic of metals).

As part of our research on the synthesis and characterization of complexes between group 12 metals and heterocyclic thiosemicarbazones, we have studied the coordination behaviour of 2-acetylpyridine 4N -phenylthiosemicarbazone (**H4PL**) and 2-acetylpyridine-*N*-oxide 4N -phenylthiosemicarbazone (**H4PLO**), in which the pyridine nitrogen, or the oxygen it bears in **H4PLO**, make it possible for the ligand to be tridentate, in contrast with the didenticity of most thiosemicarbazones.

Results and Discussion

Reaction of the thiosemicarbazones **H4PL** and **H4PLO** with Zn^{II} , Cd^{II} and Hg^{II} halides afforded the compounds listed, together with their analytical data, colours, melting points and yields, in Table 1. They all have a metal/ligand ratio of 1:1 and melting points in the range 133–302 °C (some decompose upon melting), and all are coloured, stable under air and moderately soluble in common organic solvents. In what follows we discuss their solid state IR spectra and 1H , ^{13}C and (where relevant) ^{113}Cd NMR spectra, and the

crystal structures of the ligands and of the complexes $[Cd(H4PL)Br_2] \cdot DMSO$ and $[Hg(4PL)I_2]$.

Crystal structures

Figs. 1 and 2 show the molecular structures of **H4PL** and **H4PLO**, respectively. Both adopt the Z' conformation [5], in which the C5–N bond of the pyridine ring is *trans* to the azomethine bond, as in 2-acetylpyridine 4N -methylthiosemicarbazone (**H4ML**) [6]. 4N -oxidation of **H4PL** does not significantly alter its bond lengths and angles in the solid state (Table 2). The N–N distances are less than the 1.44 Å accepted as typical of single N–N bonds, and agree well with those of similar thiosemicarbazones [6, 7]. The C–S distances are intermediate between those of single and double C–S bonds, 1.82 and 1.56 Å respectively [8], showing the partial double bond character implied by the canonical structures usually considered for thiosemicarbazones in solution [9, 10]. The azomethine bond lengths are likewise short enough to im-

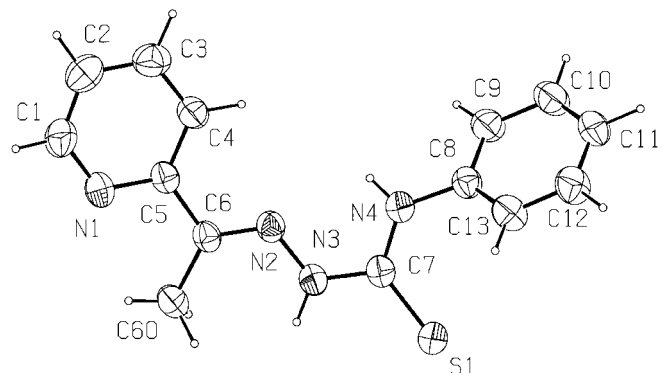


Fig. 1 Molecular structure of **H4PL** showing the atom numbering scheme. Thermal ellipsoids enclose 50% probability level. Hydrogen atoms are drawn with an arbitrary $B_{iso} = 1.5 \text{ \AA}^2$ and represented by open circles.

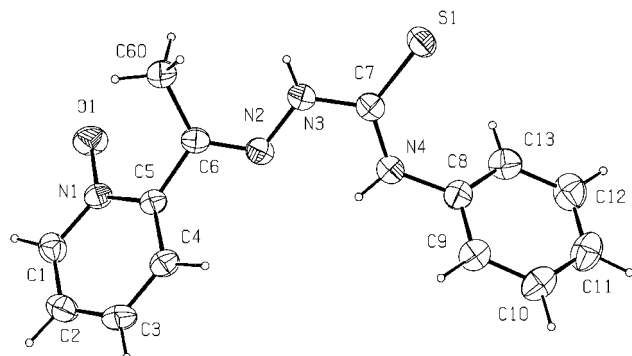


Fig. 2 Molecular structure of **H4PLO** and numbering scheme. Details as in Fig. 1.

ply a partial double bond. Although an intermolecular N–H···S bond might be expected in **H4PL**, which crystallizes in the space group $P\bar{1}$, the N···S distance measured, 3.700 Å, is well above the usual range (3.2–3.5 Å [11]). The molecular structures of **5** and of the dinuclear complex **9** are shown in Figs. 3 and 4 respectively. The chief bond lengths and angles of their ligand moieties are listed in Table 2, and those involving coordination bonds in Table 3. In both compounds the ligand is N,N,S-tridentate, coordinating via its sulphur atom and its pyridine and azomethine nitrogen atoms, and in both the metal atoms are pentacoordinate, with coordination polyhedra whose near-zero τ values [12] show them to be close to ideal tetragonal pyramids: in **5**, in which the apex of the pyramid is a bromine atom, β [N(2)–Cd(1)–Br(1)] = 139.5° and α [S(1)–Cd(1)–N(1)] = 136.1°, making τ 0.06; while in **9**, in which the apex is the sulphur atom of the monomer to which N(1) and N(2) belong, β [N(2)–Hg(1)–I(1)] = 141.8° and α [S(1)–Hg(1)–N(1)] = 140.6°, making τ 0.025.

In **9**, the two Hg atoms of the asymmetric unit are separated by 3.622 Å, and the bridging sulphur atoms by 3.858 Å. A C_2 axis perpendicular to the plane of

Table 2 Selected bond lengths (Å) and angles (°) in the bound and free thiosemicarbazone ligands

	H4PL	5 · DMSO	9	H4PLO
C(6)–N(2)	1.284(2)	1.287(10)	1.290(10)	1.284(2)
N(2)–N(3)	1.376(2)	1.352(9)	1.381(9)	1.374(2)
N(3)–C(7)	1.358(2)	1.371(10)	1.290(10)	1.361(2)
C(7)–S(1)	1.677(2)	1.677(8)	1.780(8)	1.676(2)
C(7)–N(4)	1.346(3)	1.334(10)	1.372(11)	1.337(3)
O(1)–N(1)	—	—	—	1.305(3)
N(1)–C(5)–C(4)	122.1(2)	121.1(8)	119.3(9)	—
C(4)–C(5)–C(6)	121.7(2)	122.1(7)	122.5(8)	—
N(1)–C(5)–C(6)	116.2(2)	116.9(7)	118.2(8)	117.4(2)
C(5)–C(6)–N(2)	114.9(2)	114.8(7)	117.0(8)	114.6(2)
C(6)–N(2)–N(3)	118.7(2)	120.4(6)	116.8(7)	117.3(2)
N(2)–N(3)–C(7)	118.9(2)	120.1(6)	115.7(7)	119.0(2)
N(3)–C(7)–S(1)	119.7(2)	123.5(6)	129.2(7)	119.2(1)
N(3)–C(7)–N(4)	114.8(2)	112.2(6)	119.7(7)	114.6(2)
S(1)–C(7)–N(4)	125.5(2)	124.2(6)	111.1(6)	126.2(1)
C(5)–N(1)–O(1)	—	—	—	120.1(1)
C(1)–N(1)–O(1)	—	—	—	120.1(2)

Table 3 Coordinate bond lengths (Å) and angles (°) in the complexes **5** and **9**

Parameter*	5 · DMSO	9
M–X(1)	2.563(2)	2.6786(8)
M–X(2)	2.548(2)	2.666(2)
M–S(1)	2.608(3)	2.634(2)
M–N(1)	2.363(7)	2.422(7)
M–N(2)	2.400(6)	2.412(7)
N(1)–M–X(1)	95.3(2)	100.4(2)
N(1)–M–X(2)	103.3(2)	95.8(2)
N(1)–M–N(2)	67.1(2)	67.6(2)
N(2)–M–X(1)	139.5(2)	141.7(2)
N(2)–M–X(2)	102.0(2)	97.5(2)
X(1)–M–X(2)	117.83(8)	120.3(5)
S(1)–M–X(1)	103.32(8)	107.6(5)
S(1)–M–X(2)	102.40(10)	93.43(7)
S(1)–M–N(1)	136.1(2)	140.7(2)
S(1)–M–N(2)	73.2(2)	73.3(2)

*In **5**, X(1) = Br(1), X(2) = Br(2); in **9**, X(1) = I(1), X(2) = S(1)ⁱ

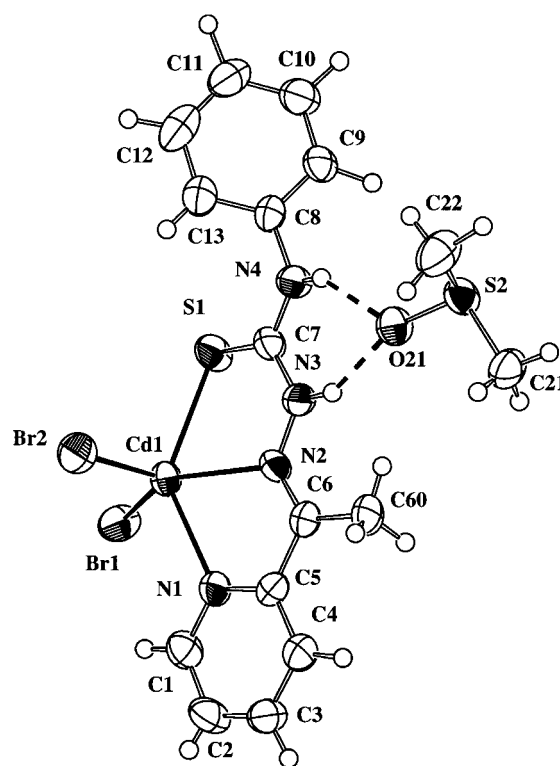
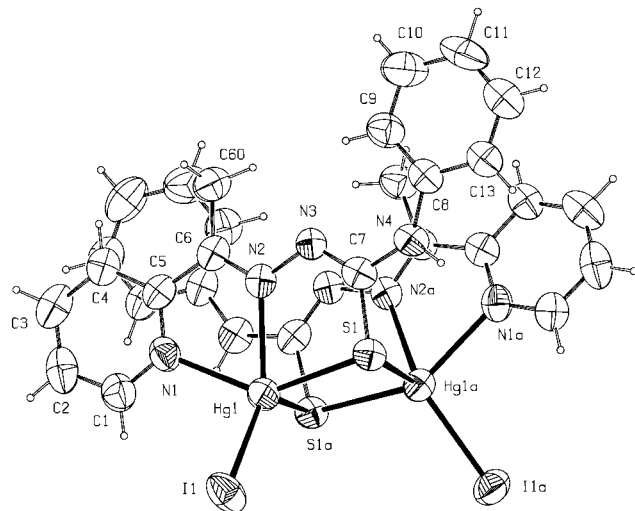


Fig. 3 Perspective view of the asymmetrical unit of the cadmium complex **5** · DMSO showing the hydrogen bonding.

the Hg₂S₂ ring means that the ligands are parallel to each other. The mean deviation of N1, N2, S' and I from the least-squares plane through the four is less than 0.02 Å, and the mercury atom lies 0.533 Å above this plane. The coordination polyhedron exhibits significant distortion: among the base plane angles with ideal values of 90°, the least deviant is S(1)–Hg(1)–I(1) [107.63(7)°] and the most deviant N(1)–Hg(1)–N(2) [67.4(4)°]. The Hg–I distance is similar to those found in other mercury complexes with terminal Hg–I bonds

**Fig. 4** Molecular structure of the dimer compound of **9**.

[13], but the bridging function of the sulphur atoms makes the Hg–S distances longer than in other complexes of mercury(II) halides with thiosemicarbazones [6, 14]. The Hg–N distances are practically identical; both are shorter than in complexes of mercury(II) with non-deprotonated thiosemicarbazones [6, 14], but are still longer than those found in many other complexes in which mercury coordinates to nitrogen [15], possibly because of their involvement in the two five-membered chelate rings of **9**. In the ligand moiety, the N(3)–C(7) bond is shorter, and the C(6)–N(2) and C(7)–S(1) bonds longer, than in the free non-deprotonated ligand. In the base of the coordination polyhedron of **5**, the angles showing minimum and maximum deviation from ideal values of 90° are respectively N(1)–Cd(1)–Br(1) [95.3(2)°] and N(1)–Cd(1)–N(2) [67.1(2)°]. The Cd–S, Cd–N and Cd–Br distances are all in the usual ranges for complexes of cadmium with thiosemicarbazones [4, 6, 14]. The bond lengths of the ligand moiety do not differ significantly from those of the free ligand, in contrast to the behaviour of the deprotonated ligand in **9**.

Infrared spectra

Table 4 lists the main IR bands of **H4PL**, **H4PLO** and their complexes in the 4000–400 cm⁻¹ region. In general, in the complexes with non-deprotonated ligands the lowest-energy $\nu(\text{N}-\text{H})$ band lies at higher frequencies, and the other two $\nu(\text{N}-\text{H})$ bands at lower frequencies, than in the free ligand; in $[\text{Hg}(\text{4PL})\text{I}]_2$, the middle band is lost due to deprotonation [16, 17] and both the others appear at slightly higher frequencies than in **H4PL**. The $\nu(\text{C}=\text{N})$ band shifts to higher frequency in all the complexes, and $\nu(\text{N}-\text{N})$ to lower frequency in most, a clear sign of coordination via the azomethine nitrogen atom [18]. Similarly, coordination via the sulphur atom is in almost all the complexes shown by a shift in $\nu(\text{C}=\text{S})$ to lower frequencies

Table 4 Main IR bands (4000–500 cm⁻¹) of the ligands and its complexes with Zn, Cd and Hg

Compound	$\nu(\text{NH})$	$\nu(\text{CN})$	$\nu(\text{NO})$	$\nu(\text{NN})$	$\nu(\text{CS})$
H4PL*	3300 s, 3243 m, 3052 w	1526 vs	—	1029 w	809 w
1	3295 m, 3229 m, 3067 w	1543 vs	—	1018 w	762 m
2	3285 m, 3227 m, 3065 m	1541 vs	—	1015 w	760 s
3	3268 m, 3214 m, 3096 m	1535 vs	—	1015 w	756 m
4	3298 w, 3225 m, 3065 m	1547 vs	—	1015 w	762 m
5	3277 m, 3219 m, 3061 m	1543 vs	—	1013 w	760 s
6	3274 m, 3208 m, 3088 m	1537 vs	—	1013 w	784 w
7	3300 w, 3232 w, 3048 m	1547 vs	—	1009 w	762 s
8	3274 w, 3216 m, 3057 m	1543 s	—	1007 w	960 s
9	3331 w, 3068 w	1534 s	—	1030 w	962 m
H4PLO	3315 m, 3016 w	1527 s	1246 m	1121 m	775 w
10	3223 w, 3119 w, 3053 w	1552 vs	1248 m	1120 w	773 w
11	3250 w, 3122 w, 3065 w	1555 vs	1240 m	1122 m	761 w
12	3259 w, 3113 w, 3061 w	1547 s	1249 m	1116 w	773 w
13	3217 w, 3059 w	1548 vs	1238 m	1114 w	775 w
14	3215 w, 3059 w	1548 vs	1238 m	1116 w	773 w
15	3221 w, 3136 w, 3063 w	1539 vs	1203 m	1116 w	761 w
16	3290 w, 3126 w, 3063 w	1537 m	1249 m	—	754 w
17	3298 w, 3124 w, 3068 w	1539 m	1257 m	—	754 w
18	3223 w, 3111 w, 3072 w	1537 vs	1263 m	1113 w	760 w

* Ref. [16]

Table 5 Main IR bands (500–100 cm⁻¹) of the ligands and its complexes with Zn, Cd and Hg, and $\nu(\text{MX})/\nu(\text{MCl})$ ratios*

Compound	$\nu(\text{MX})_{\text{as}}$	$\nu(\text{MX})_{\text{s}}$	$\nu(\text{MO})$	$\nu(\text{MN})$	$\nu(\text{MS})$	$\nu(\text{MX})/\nu(\text{MCl})$
1	282	267	—	322	—	—
2	225	200	—	319	286	0.77
3	198	179	—	325	287	0.69
4	274	245	—	318	—	—
5	194	176	—	315	283	0.71
6	166	138	—	317	282	0.58
7	261	217	—	323	—	—
8	182	154	—	312	281	0.70
9	160	144	—	328	262	0.64
				316		
10	285	235	407	—	307	—
11	221	190	420	339	302	0.77
12	195	—	411	349	314	0.68
13	256	201	416	339	317	—
14	178	142	416	337	314	0.70
15	186	137	417	330	307	0.70
16	297	—	410	337	297	—
17	203	—	421	322	275?	0.68
18	170	133	393	—	—	0.57

* Where two $\nu(\text{MX})$ bands were observed for a single complex, the mean was used.

[19]. In the complexes of **H4PL**, coordination via the pyridine nitrogen is indicated by the shifts to higher frequencies of $\nu(\text{CN}) + \nu(\text{CC})$ and of the in-plane and out-of-plane ring deformation bands: $\alpha(\text{CCC})$ is a weak band lying at 619 cm⁻¹ in **H4PL** and between 656 and 619 cm⁻¹ in its complexes, $\omega(\text{CC})$ a weak band lying at 408 cm⁻¹ in **H4PL** and between 425 and 412 cm⁻¹ in the complexes [20]. In the **H4PLO** complexes, diagnosis of coordination via the O atom on the basis of the 4000–400 cm⁻¹ spectrum is prevented by the absence of an identifiable $\delta(\text{N}-\text{O})$ band and the erratic behaviour of $\nu(\text{N}-\text{O})$, which has been described as shifting to lower frequencies upon coordination via O [21].

In the 500–100 cm⁻¹ region (Table 5), most of the complexes have bands in the ranges 260–320 cm⁻¹ and 310–350 cm⁻¹ that are absent from the spectrum of the

free ligand and are attributed to $\nu(\text{M}-\text{S})$ and $\nu(\text{M}-\text{N})$ respectively, and coordination via the O atom in the **H4PLO** complexes is shown by a band between 390 and 430 cm⁻¹ that is attributed to $\nu(\text{M}-\text{O})$. The spectra of all the complexes also show one or two bands in the sub-300 cm⁻¹ region typical of metal-halogen vibrations. As in other complexes of group 12 metal halides with thiosemicarbazones [6, 14], for a given metal and ligand, the frequencies of these bands generally exhibit the order Cl > Br > I, and for a given halogen and ligand, they generally exhibit the order Zn > Cd > Hg; the frequency ratios $\nu(\text{M}-\text{Br})/\nu(\text{M}-\text{Cl})$ and $\nu(\text{M}-\text{I})/\nu(\text{M}-\text{Cl})$ are in keeping with those reported in the literature [22].

¹H NMR spectra

The ¹H NMR signals of the ligands and complexes are listed in Table 6. Deprotonation of N3 in [Hg(4PL)I]₂ is reflected by the lack of the N3H signal that appears at 10.70 ppm in the spectrum of **H4PL**, and whose downfield shift in the other complexes reflects coordination via the azomethine nitrogen. The upfield shift of the N4H signal of some of the complexes may reflect coordination via the sulphur atom. The appearance of two N4H signals in the mercury complexes of **H4PLO**, and of two N3H signals in [Hg(H4PLO)I]₂, may be due to these complexes involving more than one isomer of the ligand; in the case of the N3H signals of [Hg(H4PLO)I]₂, an alternative explanation is the possible involvement of this proton in a hydrogen bond. The coordination of the **H4PL** complexes via their pyridine nitrogens causes their pyridine proton signals to shift much more, with respect to their positions in the free ligand spectra, than those of the **H4PLO** complexes; a similar difference has been reported between the complexes of group 12 metals

with 2-acetylpyridine ⁴*N*-dimethylthiosemicarbazone and the complexes of these metals with 2-acetylpyridine-*N*-oxide ⁴*N*-dimethylthiosemicarbazone [14].

¹³C NMR spectra

Table 7 lists the ¹³C NMR signals of the ligands and all the complexes except [Hg(4PL)I]₂, which was too insoluble for an interpretable spectrum to be obtained. Coordination of the ligand via the azomethine nitrogen is indicated in the spectra of all the complexes by the downfield shift of the methyl carbon signal, and in most (including those of all the **H4PL** complexes) by the upfield shift of the C6 signal. In the mercury complexes, coordination via the sulphur atom is indicated by the upfield shift of the C7 signal, but this signal behaves less consistently in the complexes of the other metals. Among the pyridine carbon signals, by far the most affected by complexation is that of C5, which shifts upfield in all those spectra in which it was identified; in the case of the **H4PL** complexes this may be attributed to coordination via the pyridine nitrogen, but the cause of this shift is less clear in the case of [Hg(H4PLO)Cl₂] and [Hg(H4PLO)Br₂], the only **H4PLO** complexes for which it was possible to identify this signal. The phenyl ring carbon signals lie at practically the same positions as in the free ligands.

¹¹³Cd NMR spectra

The only cadmium complexes soluble enough for a ¹¹³Cd NMR spectrum to be obtained were those of H4PL. These spectra show a single signal at 372 ppm in the chloride, 346 ppm in the bromide and 280 ppm in the iodide; the considerable breadth of all these signals may be indicative of a dynamic exchange equilibrium between the ligand and the solvent, as has been

Table 6 ¹H NMR signals of **H4PL**, **H4PLO** and their complexes with Zn, Cd and Hg (δ , ppm)

Compound	Py protons	CMe	N3H	N4H	Ph protons
H4PL	8.59(H1), 7.41(H2), 7.80(H3), 8.54(H4)	2.45	10.70	10.21	7.55(H9), 7.36(H10), 7.23(H11), 7.39(H12), 7.58(H13)
1	8.72(H1), 7.54(H2), 8.22(H3), 8.48(H4)	2.45	11.07	10.41	7.72(H9), 7.32(H10), 7.02(H11), 7.40(H12), 7.61(H13)
2	8.74(H1), 7.53(H2), 8.17(H3), 8.47(H4)	2.45	11.12	10.44	7.74(H9), 7.31(H10), 7.02(H11), 7.41(H12), 7.61(H13)
3	8.64(H1), 7.52(H2), 8.18(H3), 8.48(H4)	—	11.27	10.51	7.72(H9), 7.31(H10), 7.02(H11), 7.42(H12), 7.72(H13)
4	8.66(H1), 7.52(H2), 8.17(H3)	2.36	—	—	7.72(H9), 7.66(H13)
5	8.72(H1), 7.59(H2), 8.20(H3)	2.46	11.13	10.41	7.75(H9), 7.40(H10), 7.20(H11), 7.42(H12), 7.59(H13)
6	8.74(H1), 7.59(H2), 8.20(H3)	2.46	11.16	10.43	7.78(H9), 7.40(H10), 7.21(H11), 7.42(H12), 7.59(H13)
7	8.77(H1), 7.54(H2), 8.12(H3), 8.47(H4)	—	10.81	9.90	7.69(H9), 7.37(H10), 7.18(H11), 7.43(H12), 7.58(H13)
8	8.74(H1), 7.57(H2), 8.11(H3), 8.43(H4)	2.48	10.70	9.91	7.67(H9), 7.38(H10), 7.18(H11), 7.38(H12), 7.60(H13)
9	8.72(H1), 7.60(H2), 8.11(H3), 8.46(H4)	—	—	—	7.70(H9), 7.37(H10), 7.37(H12), 7.39(H13)
H4PLO	8.28(H1), 7.40(H2), 7.45(H3), 7.75(H4)	2.33	10.88	10.09	7.52(H9), 7.34(H10), 7.18(H11), 7.36(H12), 7.54(H13)
10	8.31(H1), 7.47(H3), 7.79(H4)	2.34	10.88	10.06	7.53(H9), 7.32(H10), 7.16(H11), 7.32(H12), 7.53(H13)
11	8.33(H1), 7.80(H4)	2.35	10.88	10.06	7.53(H9), 7.32(H10), 7.16(H11), 7.32(H12), 7.53(H13)
12	8.34(H1), 7.83(H4)	2.36	10.88	10.05	7.53(H9), 7.32(H10), 7.16(H11), 7.32(H12), 7.53(H13)
13	8.29(H1), 7.41(H2), 7.60(H4)	2.30	10.67	9.91	7.32(H9), 7.15(H10), 7.32(H11)
14	8.29(H1), 7.46(H3), 7.78(H4)	2.33	10.86	10.08	7.50(H9), 7.32(H10), 7.16(H11), 7.32(H12), 7.50(H13)
15	8.30(H1), 7.44(H3), 7.79(H4)	2.34	10.85	10.06	7.51(H9), 7.33(H10), 7.16(H11), 7.33(H12), 7.51(H13)
16	8.46, 8.38(H1), 7.65(H3), 7.81, 7.74(H4)	2.30	10.85	9.73	7.49(H9), 7.34(H10), 7.14(H11), 7.34(H12), 7.49(H13)
17	8.48, 8.39(H1), 7.83(H4)	—	10.73	9.74	7.51(H9), 7.34(H10), 7.13(H11), 7.34(H12), 7.51(H13)
18	8.46, 8.39(H1), 7.66(H3), 7.83(H4)	—	10.92	9.79	7.48(H9), 7.33(H10), 7.14(H11), 7.33(H12), 7.48(H13)
			10.57	9.60	

Table 7 ^{13}C NMR signals of **H4PL**, **H4PLO** and their complexes with Zn, Cd and Hg (δ , ppm)

Compound	C1	C2	C3	C4	C5	C6	C60	C7	C8	C13 C9	C12 C10	C11
H4PL	149.38	121.46	136.58	125.78	154.71	148.67	12.73	177.46	139.35	126.41	128.33	124.32
1	148.59	121.14	138.78	125.66	150.68	145.51	14.02–13.02	177.36–175.93	140.74	126.35	128.45	123.49
2	148.67	121.17	138.75	125.70	150.17	145.23	14.07–13.07	177.38–175.92	140.81	126.37	128.79	123.49
3	148.54	121.50	138.77	124.93	–	–	14.31	175.85	140.38	126.30	128.79	123.47
4	148.66	121.33	137.61	124.09	149.37	–	14.79–12.95	177.74	140.69	126.50	–	–
5	148.25	123.01	138.58	125.06	149.12	144.87	14.46–13.42	176.89–176.18	140.59	126.18	128.77	123.99
6	148.05	123.21	138.75	125.39	149.01	143.14	14.70–13.64	176.25	140.82	126.31	128.98	124.31
7	148.95	121.54	138.10	127.19	–	–	14.22–13.97	175.00	139.94	125.97	128.89	124.05
8	148.86	121.49	–	–	–	145.50	–	–	139.84	125.96	128.84	124.09
H4PLO	147.26	125.58	139.16	127.56	156.00	146.00	16.46	177.62	139.79	125.93	128.32	126.79
10	147.17	125.39	139.12	127.68	–	145.86	16.58	177.69	139.91	125.82	128.35	126.75
11	147.15	125.39	139.10	127.73	–	145.84	16.69	177.66	140.01	–	128.38	126.76
12	–	125.40	139.09	127.78	–	145.75	16.69	177.71	140.01	126.78	128.39	127.30
13	147.14	125.35	139.11	127.57	–	146.19	16.60	177.41	139.87	125.87	128.34	126.78
14	146.98	125.78	139.10	127.64	–	146.17	16.69	177.40	139.94	126.67	128.35	127.18
15	–	125.35	139.15	127.63	–	146.22	16.69	177.52	139.95	125.88	128.36	–
16	–	125.34	137.99	127.59	151.87	145.43	16.90	161.22	138.40	126.54	128.23	126.92
17	147.21	124.92	138.66	127.25	153.45	146.61	18.79	174.46	139.91	125.53	128.76	126.72
18	–	–	–	127.24	–	–	17.68	–	139.95	–	128.72	–

Table 8 Antifungal activity of $[\text{Hg}(\text{H4PLO})\text{I}_2]$. Concentration ($\mu\text{g mL}^{-1}$)

	100 ^{a)}	200	400	600	1000
<i>Aspergillus niger</i> $[\text{Hg}(\text{H4PLO})\text{I}_2]$	6.3	8.5	8.8	10.5	11.0
Nystatin ^{b)}	–	9.0	10.7	12.8	17.3
<i>Paecilomyces variotii</i> $[\text{Hg}(\text{H4PLO})\text{I}_2]$	6.0	8.3	9.3	11.0	13.0
Nystatin	–	12.8	14.5	16.5	25.2

^{a)} Diameter of growth inhibition zone (6.0 indicates no inhibition);^{b)} Commercially available therapeutic agent.

suggested previously for this kind of system [4]. All three signals show the nuclide to be less shielded than in $\text{Cd}(\text{ClO}_4)_2$, the standard. In the chloro complex the Cd nucleus is less shielded than in CdCl_2 , but in the bromo and iodo complexes it is more shielded than in DMSO solutions of CdBr_2 and CdI_2 respectively [23]. The chemical shifts of the bromo and iodo complexes are very similar to those of the corresponding cadmium dihalide complexes of H4ML [6], but that of the chloro complex is greater than in the complex with the less bulky ^4N -substituent.

Antifungal activity

The antifungal activity of all the new compounds was assayed against the pathogenic fungi *Aspergillus niger* and *Paecilomyces variotii*. Only $[\text{Hg}(\text{H4PLO})\text{I}_2]$ exhibited any activity (Table 8). Though less active than the commercially available antifungal agent nystatin, $[\text{Hg}(\text{H4PLO})\text{I}_2]$ was more active than complexes of group 12 metal halides with 2-acetylpyridine-*N*-oxide- ^4N -dimethylthiosemicarbazone, in which the ^4N -substituents are less bulky than the phenyl group [14].

Experimental Part

Elemental analyses (C, N, H) were performed with a Carlo Erba 1108 microanalyser. Melting points were determined in

a Büchi apparatus. IR spectra were recorded on a Mattson Instruments Cygnus 100 FTIR spectrometer using KBr pellets for spectra run from 4000 to 400 cm^{-1} and polyethylene-sandwiched Nujol mulls for the range 500–100 cm^{-1} . ^1H and ^{13}C NMR spectra in $(\text{CD}_3)_2\text{SO}$ were recorded on a Brucker WM-300 spectrometer with TMS as internal reference. ^{113}Cd NMR spectra of 10^{-2} M solutions in DMSO were run on a Brucker WM-250 spectrometer and referred to 0.1 M $\text{Cd}(\text{ClO}_4)_2$.

Reagents [2-acetylpyridine, 4-phenyl-3-thiosemicarbazide, ZnBr_2 , $\text{CdCl}_2 \cdot \text{H}_2\text{O}$, $\text{CdBr}_2 \cdot 4\text{H}_2\text{O}$, CdI_2 , HgBr_2 and HgI_2 (all from Aldrich), HgCl_2 (from Merck), and ZnCl_2 and ZnI_2 (both from Ventron)] were all used without prior purification. 2-Acetylpyridine-*N*-oxide was prepared by oxidation of 2-acetylpyridine with hydrogen peroxide as per Winterfield and Zickel [24]. The ligands were prepared using Klayman *et al.*'s [25] general method for condensation of amines with aldehydes or ketones, as follows.

2-Acetylpyridine-4-N-phenylthiosemicarbazone (H4PL). A solution of 2-acetylpyridine (10.80 g, 0.089 mol) in 50 mL of ethanol was slowly added to a solution of 4-phenyl-3-thiosemicarbazide (14.91 g, 0.089 mol) in 100 mL of hot water. After refluxing for 2 h, the yellow product was filtered out, and recrystallization from ethanol afforded crystals suitable for X-ray diffraction studies. Yield, 96%. Mp. 190 °C. $\text{C}_{14}\text{H}_{14}\text{N}_4\text{S}$ (270.09): C, 62.3 (calc. 62.2); H, 5.2 (5.2); N, 20.7 (20.7)%. MS-FAB (m/z , %): $[\text{L} + \text{H}]^+$, 271(100).

2-Acetylpyridine-*N*-oxide-4-N-phenylthiosemicarbazone (H4PLO). **H4PLO** was synthesized by a procedure analogous to that described above for **H4PL**, but starting from 2-acetylpyridine-*N*-oxide. Crystals suitable for X-ray diffraction studies were obtained upon storing the mother liquor of the recrystallization step at low temperature. Yield, 85%. Mp. 185 °C. $\text{C}_{14}\text{H}_{14}\text{N}_4\text{OS}$ (286.08): C, 58.4 (calc. 58.7); H, 5.2 (4.9); N, 19.6 (19.6)%. MS-FAB (m/z , %): $[\text{L} + \text{H}]^+$, 287(100); $[\text{L}]^+$, 286(16).

Preparation of the thiosemicarbazone metal(II) complexes. To a solution of the appropriate thiosemicarbazone in hot ethanol was added an equimolar amount of the appropriate metal salt dissolved or suspended in ethanol. The mixture was stirred for about 1 week, and the coloured solids formed

Table 9 Crystal and structure refinement data for the ligands H4PL and H4PLO, and its complexes **5** and **9**

Compound	H4PL	5 · DMSO	9	H4PLO
Empirical formula	C ₁₄ H ₁₄ N ₄ S	C ₁₆ H ₂₀ Br ₂ CdN ₄ OS ₂	C ₂₈ H ₂₆ Hg ₂ I ₂ N ₈ S ₂	C ₁₄ H ₁₄ N ₄ OS
Formula weight	270.35	620.71	1193.67	286.35
Wavelength/Å	0.71073	0.71073	0.71073	1.54184
Crystal size/mm	0.35 × 0.20 × 0.15	0.90 × 0.90 × 0.10	0.25 × 0.15 × 0.10	0.10 × 0.10 × 0.10
Crystal shape	prism	plate	prism	prism
Crystal system	Triclinic	Triclinic	Monoclinic	Monoclinic
Space group	P $\bar{1}$ (No. 2)	P $\bar{1}$ (No. 2)	C ₂ /c (No. 15)	P ₂ / ₁ c (No. 14)
<i>a</i> /Å	10.155(3)	9.057(8)	18.518(4)	7.202(1)
<i>b</i> /Å	11.614(4)	12.196(1)	16.838(2)	23.785(1)
<i>c</i> /Å	5.860(1)	9.991(1)	14.569(4)	8.564(2)
α /°	91.76(2)	90.35(6)	90.00(–)	90.00(–)
β /°	90.99(2)	100.89(5)	131.896(9)	111.50(1)
γ /°	76.31(2)	91.28(6)	90.00(–)	90.00(–)
<i>V</i> /Å ³	671.1(3)	1083.4(18)	3381.5(12)	1364.1(4)
<i>Z</i> , <i>D</i> _{calcd} /Mg/m ³	2, 1.338	2, 1.903	4, 2.345	4, 1.394
<i>F</i> (000)	284	604	2192	600
θ range/°	3.05–29.94	3.23–28.70	3.06–30.94	5.86–69.97
Temperature/K	293	213	293	213
<i>l</i> _{min} / <i>l</i> _{max}	–14/14	–1/12	–26/19	–1/7
<i>k</i> _{min} / <i>k</i> _{max}	–16/16	–16/16	0/24	0/28
<i>l</i> _{min} / <i>l</i> _{max}	0/8	–13/13	0/21	–10/10
μ /mm ^{–1}	0.232	4.90	11.050	2.121
Max./min. transmissions	0.482/0.054	0.999/0.616	0.401/0.026	0.666/0.197
Refl. collected/unique	4243/3891	6664/5633	5550/5364	3090/2450
Data/parameters	3891/228	5631/280	5364/191	2450/237
Final <i>R</i>	0.063	0.071	0.053	0.040
Final <i>wR</i> 2	0.170	0.175	0.104	0.106
GOOF	1.058	1.101	0.988	1.023
Max. $\Delta\rho$ /eÅ ^{–3}	0.508	1.740	1.456	0.262

were filtered out, washed with ethanol and vacuum dried. Single crystals of **9** suitable for X-ray diffraction studies were obtained by slow evaporation of solvent from the filtrate, and single crystals of **5 · DMSO** by recrystallization from DMSO.

Crystallographic Section

Crystals of **H4PL**, **5 · DMSO**, **9** and **H4PLO** suitable for X-ray diffraction were mounted on glass fibers and transferred to an Enraf Nonius CAD4 diffractometer. Accurate unit-cell parameters and an orientation matrix were determined by least-squares refinement of the setting angles of a set of well-centered reflections (SET4) [26] in the range 8.1–15.3 (**H4PL**), 7.1–13.6 (**5 · DMSO**), 8.3–13.5 (**9**) and 17.5–26.4 (**H4PLO**). Reduced-cell calculations did not indicate higher lattice symmetry [27]. Crystal data and details of the data collection and refinement are given in Table 9. Data were corrected for Lp effects and for observed linear decay of the reference reflections. An empirical absorption correction (DIFABS) [28] was applied for all compounds. The structures were solved by automated Patterson or direct methods and subsequent difference Fourier techniques (SHELXS86) [29] and refined on *F* (SDP/VAX) [30] or *F*² (SHELXL97) [31] by a full-matrix least-squares procedure using anisotropic displacement parameters. Hydrogen atoms were located from difference Fourier maps and refined isotropically in **H4PL**, **H4PLO**, **5 · DMSO**, or were included in the refinement in calculated positions riding on their carried atoms in **9**. Neutral atom scattering factors and anomalous dispersion corrections were taken from the International Tables for X-Ray Crystallography [32]. Geometrical calculations and illustrations were performed with SHELXL97 [31], ZORTEP [33] and PLATON98 [34] package. Further details

of the crystal structure determination can be ordered from Fachinformationszentrum Karlsruhe GmbH, D-76344 Eggenstein-Leopoldshafen (Germany), under the depository numbers CSD-410603 to CSD-410606.

References

- [1] E. S. Raper, *Coord. Chem. Rev.* **1985**, *61*, 115; D. X. West, S. B. Padhye, P. B. Sonawane, *Structure and bonding* **1991**, *76*, 4.
- [2] J. S. Casas, M. V. Castaño, M. C. Argüelles, A. Sánchez, J. Sordo, *J. Chem. Soc. Dalton Trans.* **1993**, 1253.
- [3] J. S. Casas, E. E. Castellano, A. Macías, M. C. Argüelles, A. Sánchez, J. Sordo, *J. Chem. Soc. Dalton Trans.* **1993**, 755.
- [4] J. S. Casas, M. V. Castaño, M. S. García-Tasende, I. Martínez-Santamaría, J. Sordo, E. E. Castellano, J. Zukerman-Schpector, *J. Chem. Res.* **1992**, 324.
- [5] D. X. West, G. A. Bain, R. J. Butcher, J. P. Jasinski, Y. Li, R. Y. Pozdniakov, J. Valdés-Martínez, R. A. Toscano, S. Hernández-Ortega, *Polyhedron* **1996**, *15*, 665.
- [6] E. Bermejo, R. Carballo, A. Castañeras, R. Domínguez, A. E. Liberta, C. Maichle-Mössmer, M. M. Salberg, D. X. West, *Eur. J. Inorg. Chem.* **1999**, in press.
- [7] J. Palenik, D. F. Rendle, W. S. Carter, *Acta Crystallogr.* **1974**, *B30*, 2390.
- [8] L. E. Sutton, *Tables of Interatomic Distances and Configuration in Molecules and Ions*. Supplement, The Chemical Society, London, 1965.
- [9] D. X. West, B. L. Monkiewski, H. Gebremedhin, T. J. Romack, *Transition Met. Chem.* **1992**, *17*, 384.
- [10] D. Kovala-Demertzis, A. Domopoulos, M. Demertzis, C. P. Raptopoulou, A. Terzis, *Polyhedron* **1994**, *13*, 1917.

- [11] R. Srinivasan, K. K. Chacko, *Conformation of Biopolymers*, Vol. 2, Academic Press, New York, 1967.
- [12] A. W. Addison, T. N. Rao, J. Reedijk, J. van Rijn, G. C. Verschoor, *J. Chem. Soc. Dalton Trans.* **1984**, 1349.
- [13] A. Castiñeiras, A. Arquero, J. R. Masaguer, S. Martínez-Carrera, S. García-Blanco, *Z. Anorg. Allg. Chem.* **1986**, 539, 219.
- [14] E. Bermejo, R. Carballo, A. Castiñeiras, R. Domínguez, A. E. Liberta, C. Maichle-Mössmer, D. X. West, *Z. Naturforsch.* **1999**, in press.
- [15] A. G. Orpen, L. Brammer, F. H. Allen, O. Kennard, D. G. Watson, R. Taylor, *J. Chem. Soc. Dalton Trans.* **1989**, 51.
- [16] S. K. Jain, B. S. Garg, Y. K. Bhoon, D. L. Klayman, J. P. Scovill, *Spectrochim. Acta* **1985**, 41A, 407.
- [17] M. F. Iskander, I. El-Sayed, *J. Inorg. Nucl. Chem.* **1971**, 33, 4253.
- [18] R. C. Aggarwal, T. Prasad, B. N. Yadav, *J. Inorg. Nucl. Chem.* **1975**, 37, 899.
- [19] A. Castiñeiras, A. Arquero, J. R. Masaguer, *Transition Met. Chem.* **1984**, 9, 273.
- [20] C. Airoldi, A. S. Gonçalves, *J. Inorg. Nucl. Chem.* **1978**, 40, 1817.
- [21] R. G. Garvey, J. H. Nelson, R. O. Ragsdale, *Coord. Chem. Rev.* **1968**, 3, 375.
- [22] R. J. H. Clark, C. S. Williams, *Inorg. Chem.* **1965**, 4, 350; G. B. Deacon, J. H. S. Green, D. J. Harrison, *Spectrochim. Acta* **1968**, 24A, 1921.
- [23] T. Drakenberg, N.-O. Björk, R. Portanova, *J. Phys. Chem.* **1978**, 82, 2423.
- [24] K. Winterfeld, W. Zickel, *Arch. Pharm. (Weinheim, Ger.)* **1969**, 302, 900.
- [25] D. L. Klayman, J. F. Bartosevich, T. S. Griffin, C. J. Mason, J. P. Scovill, *J. Med. Chem.* **1979**, 22, 855; D. L. Klayman, J. P. Scovill, J. F. Bartosevich, C. J. Mason, *J. Med. Chem.* **1979**, 22, 1367; J. P. Scovill, D. L. Klayman, C. F. Franchino, *J. Med. Chem.* **1982**, 25, 1261; D. L. Klayman, J. P. Scovill, J. F. Bartosevich, J. Bruce, *J. Med. Chem.* **1983**, 26, 35; J. P. Scovill, D. L. Klayman, C. Lambross, G. E. Childs, J. D. Notsch, *J. Med. Chem.* **1986**, 27, 87.
- [26] J. L. de Boer, A. J. M. Duisenberg, *Acta Crystallogr.* **1984**, A40, 410.
- [27] A. L. Spek, *J. Appl. Cryst.* **1988**, 21, 578.
- [28] N. Walker, D. Stuart, *Acta Crystallogr.* **1983**, A39, 158.
- [29] G. M. Sheldrick, SHELLXS86, Universität Göttingen, 1986.
- [30] B. A. Frenz and Associates Ins. & Enraf-Nonius. VAX/SDP Structure Determination Package, vers. 2.2, College Station, Texas, USA (1986).
- [31] G. M. Sheldrick, SHELLXSL97, Universität Göttingen, 1997.
- [32] A. J. C. Wilson, *International Tables for Crystallography*, Vol. C, Kluwer Academic Publishers, Dordrecht, The Netherlands, 1992.
- [33] L. Zsolnai, ZORTEP, Universität Heidelberg, 1997.
- [34] A. L. Spek, *Acta Crystallogr.* **1990**, A46, C34.